J BONE ONCOL 51 (2025) 100666

Contents lists available at ScienceDirect

Journal of Bone Oncology

journal homepage: www.elsevier.com/locate/jbo

Research Paper

Feasibility of ADC histogram analysis for predicting of postoperative recurrence in aggressive spinal tumors

Qizheng Wang [a,1], Yongye Chen [a,1], Guangjin Zhou [a,1], Tongyu Wang [b], Jingchao Fang [a], Ke Liu [a], Siyuan Qin [a], Weili Zhao [a], Dapeng Hao [b], Ning Lang [a,*]

[a] Department of Radiology, Peking University Third Hospital, 49 North Garden Road, Haidian District 100069 Beijing, PR China
[b] Department of Radiology, the Affiliated Hospital of Qingdao University, No. 16 Jiangsu Rd, Qingdao 266000 Shandong, PR China

HIGHLIGHTS

- As potential biomarkers, ADC histogram metrics were promising to predict spinal tumor recurrence.
- Skewness, mean and 50th percentiles ofADC from pretreatment MRI were independent predictors.
- The ADC histogram prediction model performed better than the clinical prediction model.

GRAPHICAL ABSTRACT

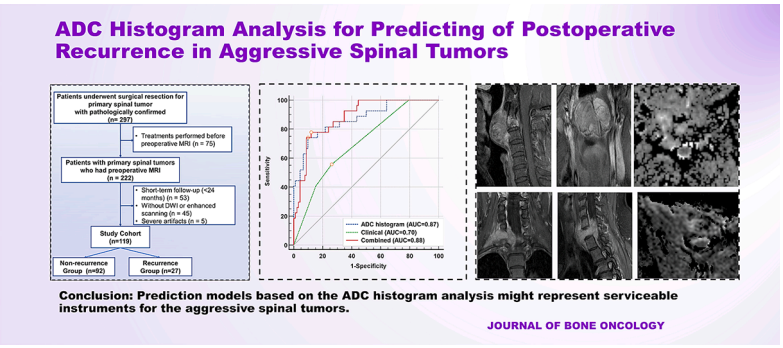

ARTICLE INFO

Keywords:
Diffusion weighted imaging
Spinal tumor
Recurrence
Histogram analysis

ABSTRACT

Background: Risk stratification of spinal tumors is a major unmet clinical need for personalized therapy.
Purpose: To explore the feasibility of pretreatment whole-lesion apparent diffusion coefficient (ADC) histogram in predicting local recurrence of aggressive spinal tumors.
Methods: 119 aggressive spinal tumor patients (median age, 40; range, 13–74 years) confirmed by pathological findings with a mean follow-up of 36 months were enrolled and divided into the recurrence and non-recurrence group. The histogram metrics of whole-lesion, including the maximum, mean, kurtosis, skewness, entropy, and percentiles (10th, 25th, 50th, 75th, 95th) ADC values, were evaluated and take the average. Fractal dimension (FD) was assessed in the three orthogonal directions and take maximum. Clinical and general imaging features were used to construct an alternative prognostic model for comparison. Variables with statistical differences would be included in stepwise logistic regression analysis.
Results: As for the clinical model, Enneking staging (odds ratio [OR]: 3.572; $P = 0.04$) and vertebral compression (OR: 4.302; $P = 0.002$) were independent predictors of recurrence. There was no statistical difference in FD between the two groups ($P = 0.623$). Among the ADC histogram parameters compared, skewness, maximum, and

Abbreviations: DWI, Diffusion weighted imaging; ADC, Apparent diffusion coefficient; ICD, International classification of diseases; FD, Fractal dimension; ROC, Receiver operating characteristic curves; AUC, Area under curve; CI, Confidence interval; OR, Odds ratio.

* Corresponding author at: Peking University Third Hospital, Department of Radiology, 49 North Garden Road, Haidian District, Beijing 100191, PR China.
E-mail address: langning800129@126.com (N. Lang).

[1] These authors contributed equally to this paper.

https://doi.org/10.1016/j.jbo.2025.100666
Received 14 October 2024; Received in revised form 10 February 2025; Accepted 10 February 2025
Available online 11 February 2025

mean ADC values were independent risk factors and constructed ADC histogram prediction models. The ADC histogram model (AUC = 0.871) and the combined model (AUC = 0.884) performed better than the clinical prediction model (AUC = 0.704) with *P*-values of 0.004 and 0.001, respectively.
Conclusion: Prediction models based on the ADC histogram analysis might represent serviceable instruments for the aggressive spinal tumors.

1. Introduction

Primary bone tumors of the spine, though rare, might significantly impact patients' quality of life. Primary spinal tumors require careful clinical management because of their close-proximity to important neurovascular structures, yet they represent a difficult treatment paradigm [1–3]. According to the World Health Organization classification of bone tumors, aggressive tumors include intermediate (including locally aggressive and rarely metastasizing) and malignant. Stratification of recurrence risk in patients with aggressive spinal tumors may aid clinical decision making to improve prognosis, which is a major unmet clinical need [4]. Patients with a high risk of recurrence should be treated with a more thorough surgical approach, and if feasible, adjuvant therapy and closer postoperative follow-up should be considered. Early prediction of relapse is expected to help reduce under-treatment or over-treatment and improve patient outcomes through optimized decision making.

With its high tissue resolution and powerful functional imaging capabilities, MRI is an excellent preoperative tool to preoperatively evaluate spinal tumors. Diffusion-weighted imaging (DWI) and corresponding quantitative apparent diffusion coefficient (ADC) maps are commonly used functional imaging techniques, which can reveal the microscopic changes to the cellular environment of tumors. Meanwhile, quantitative approaches to tumor MRI using ADC histograms have gained popularity, which have been shown to correspond to tumor markers, resulting in improved diagnostic performance in the evaluation of multiple tumors [5–8]. However, this approach has not yet been studied in risk stratification of spinal tumors.

Previous studies have also shown that clinical features, such as age, vertebral compression, multiple vertebral involvement, and Enneking stage, might be associated with postoperative recurrence of spinal tumors [9–12]. For quantitative evaluation of tumor morphology, fractal analysis using fractal geometry is considered to describe the structures of focal lesions, making it possible to modeled irregular tumor structures [13]. Indeed, some studies have shown that fractal analysis can be used to identify focal lesions, including but not limited to cardiomyopathy, pancreatic ductal adenocarcinoma, gastrointestinal tumors [14–17]. To the best of our knowledge, whether fractal dimensions contribute to the recurrence prediction of spinal tumors has not been studied.

Consequently, this study aimed to evaluate the utility of clinical factors combined with potential quantitative MRI biomarkers (fractal analysis and volumetric ADC histograms) to characterize primary aggressive spinal tumors.

2. Materials and methods

2.1. Selection of patients

This retrospective study from two institutions was approved by the Ethics review board and informed consent was waived (M2023827). The study was carried out following the tenets of the Declaration of Helsinki.

Medical records of 297 patients with localized primary spinal tumors who attended our institution from September 2010 to June 2022 were identified. Among them, 178 patients were excluded because (1) Treatments were performed before preoperative MRI (n = 75); (2) short-term follow-up (<24 months) (n = 53); (3) no DWI or enhanced scanning (n = 45), and (4) severe artifacts in the ADC map (n = 5). Finally, 119 patients with localized primary spinal tumors were enrolled as the study cohort. Fig. 1 details the inclusion and exclusion criteria.

2.2. Postoperative follow-up and clinical outcome

Data regarding the disease course of the patients with spinal tumors were collected from their medical records. All patients followed the standardized clinical follow-up guidelines after spinal tumor surgery, which was conducted every 3 months for the first 2 years, every 6 months for 3–5 years, and annually after 5 years, including CT and MRI scans. Final follow-up occurred on the 30th of June 2024. Imaging (CT, MRI, or positron emission tomography) and/or tissue biopsy were used to confirm local recurrence within the follow-up period. Patients with no evidence of recurrence during the follow-up period (at least 24 months) were classified into the no-recurrence group.

2.3. MRI protocols

Two 3.0T scanners (GE Discovery 750WS; GE Signa HDxt) used body-phased array coils to carry out the MRI examinations at two institutions. We obtained the following pulse sequences: T2-weighted fat-saturation fast-recovery fast spin echo; T1 and T2-weighted gradient echo; and DWI sequences (b0 together with various gradients chosen from 50, 200, 400, 600, 800, 1000, 1200 and 1500 s/mm^2). For the lesions, contrast enhanced-MRI was carried out using a three-dimensional volume interpolated breath-hold examination transverse scan. Gadopentetate dimeglumine, as the contrast agent, was administered at 0.1 mmol/kg (flow rate of 2 ml/s) using an Ulrich power injector. A senior technician (G.Z.) verified the scanning parameters and image quality. The overall scanning time (including routine scan sequence; DWI; Enhanced scanning) was ranged from 24 min 30 s to 27 min. The variation in the number of layers required was contingent upon the size of the tumor.

2.4. Pathological and routine imaging characteristics

Pathological and routine imaging characteristics were evaluated by two trained observers (K.L.&W.Z.). During curative resection, surgical specimens were obtained from all enrolled patients, which were used for histopathological evaluation. Enneking staging was extracted from patient data and divided into two stages (Intra-compartmental / Extra-compartmental) [18]. The general imaging features of spinal tumor lesions included tumor location, vertebral compression, and multi-vertebral involvement, were recorded follow the routine diagnostic procedure.

2.5. Fractal dimension analysis

Fractal analysis applies nontraditional mathematics to patterns that are difficult to comprehend using traditional Euclidean concepts. The fractal dimension (FD) is calculated using the box-counting algorithm, which represents the complexity or roughness of a binary mask surface [19]. The FracLac version 2.5 plugin of ImageJ (NIH, Bethesda, MD, USA), downloaded from https://imagej.nih.gov/ij/plugins/fraclac/FLHelp/Images.htm, was used for FD analysis.

The FD can be obtained mathematically using:

$$FD = \lim_{\epsilon \to 0} \frac{log(N(\epsilon))}{log(1/\epsilon)}, \quad (1)$$

where ∈ is a box size and $N(\in)$ is the number of counted boxes. The measurement was performed manually by two junior radiologists (Q. W.&Y.C.) and 8-bit binary images were converted and generated for FD determination. Take the maximum value after measuring in three orthogonal directions. Slice selection and delineation of the region of interest were supervised by a senior radiologist (N.L.). Finally, the two radiologists' measurements were averaged as the fractal dimension of tumor. The image processing applied to each case to analyze tumor heterogeneity is shown in Fig. 1.

2.6. ADC histogram analysis

ADC maps were generated generation using a mono-exponential decay model in a post-processing console (Advantage Windows). Two radiologists (Q.W.&Y.C.) with five years of experience in musculoskeletal imaging carried out the ADC Histogram analysis. Whole lesion regions of interest were manually drawn along the tumour border layer by layer on the ADC (b = 1500 s/mm^2) map using Firevoxel (FireVoxel medical image processing, https://www.FireVoxel.org). In the process of annotation, T1WI, T2WI and CE-MRI images can be referenced simultaneously to ensure the accuracy of sketching as much as possible. Then, the following histogram features were extracted automatically: skewness, kurtosis, and entropy, max-ADC, mean-ADC, 10th percentile, 25th percentile, 50th percentile, 75th percentile, and 90th percentile of the ADC, expressed as 10^{-6} mm^2/s. ADC quantifies the diffusivity of water molecules within tissues, serving as a crucial biomarker for tumor characterization. Lower ADC values generally indicate restricted diffusion, which is often associated with increased cellular density and malignancy. Skewness describes the asymmetry of the ADC value distribution, where a positive skew suggests a rightward tail, and a negative skew indicates a leftward tail, potentially reflecting variations in tumor composition. Kurtosis measures the sharpness of the ADC distribution peak, with higher kurtosis values suggesting a more heterogeneous tissue microstructure, which may correlate with tumor aggressiveness. Entropy quantifies the complexity and heterogeneity of the ADC distribution, with higher entropy values indicative of a more disordered and heterogeneous tumor microenvironment. These radiomic features provide valuable insights into the structural and pathological characteristics of spinal tumors, aiding in their differentiation and prognostication. Fig. 1 depicts the study workflow, with example delineations.

2.7. Statistical analysis

MedCalc Statistical software (Version 16.8) and GraphPad Prism software (Version 10.1.2) were used to carry out all the statistical analyses. The Shapiro-Wilk test was used to check data distribution. Mann–Whitney's *U* tests (for continuous variables) and the chi-squared test (for categorical variables) were used to compare the parameters and characteristics of the recurrence and non-recurrence groups. Interobserver agreement was evaluated by intraclass correlation coefficient (ICC): excellent, 0.81–1.00; moderate, 0.61–0.80; fair, 0.21–0.40; poor, 0–0.20. Clinical characteristics and ADC histogram parameters with $P < 0.1$ were included in the logistic regression analysis using forward linear regression. Receiver operating characteristic curves (ROC) were used to evaluate the diagnostic performances of different risk stratification methods. The area under the curve (AUC) were calculated and compared by DeLong test. Statistical significance was considered at $P < 0.05$ (two-tailed).

3. Results

3.1. Patients' characteristics

The 119 patients with aggressive spinal tumors met the inclusion criteria (median age: 40 years, range: 13–74 years. Pathological types include chordoma (n = 40), giant cell tumor of bone (n = 30), chondrosarcoma (n = 21), osteoblastoma (n = 8), osteosarcoma (n = 8), Ewing's sarcoma (n = 4), hemangiosarcoma (n = 5), and other rare sarcoma types (n = 3). In the study cohort, 27 (22.7 %) cases of recurrence were observed during a mean follow-up period of 36.0 months (range = 28.5–56 months). The characteristics of patients are shown in Table 1.

3.2. Group differences

Table 2 shows the comparison of pretreatment characteristics between the recurrence and non-recurrence groups. Univariate analysis showed that the no differences were observed for age, gender, Enneking stage, and multi-vertebral involvement. The FD in the recurrence group was slightly larger than the recurrence group without statistical difference (recurrence, median = 1.30; range 1.01–1.63 *vs.* non-recurrence, median = 1.32, range 1.06–1.50, $P = 0.623$). Among the ADC histogram parameters compared, skewness ($P = 0.019$) and kurtosis ($P = 0.003$) were significantly different between the recurrence and non-recurrence groups. No significant differences were detected for

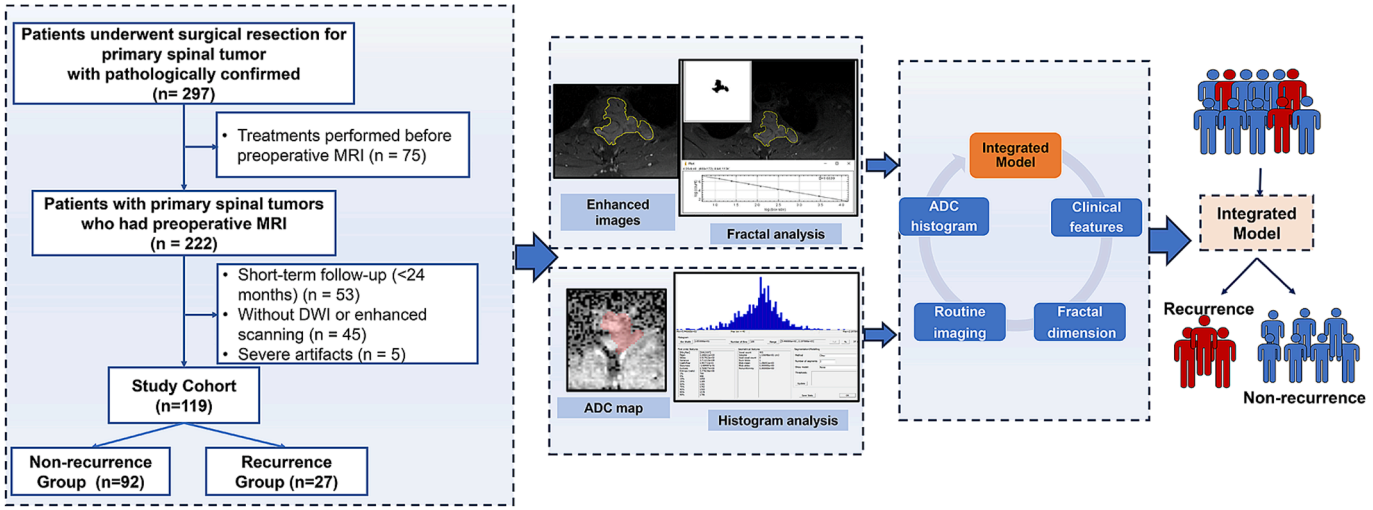

Fig. 1. The workflow of the study.

Table 1
Clinical and pathological characteristics of patients in study cohorts.

Characteristics	Total (N = 119)
Gender	
Male	67 (56.3 %)
Female	52 (43.7 %)
Age at surgery	
Median (IQR)	40 (27.0 – 55.0)
Location	
Cervical	16 (13.4 %)
Thoracic	45 (37.8 %)
Lumbar	27 (22.7 %)
Sacrococcygeal	31 (26.1 %)
Enneking stage	
Intra-compartmental	33 (27.7 %)
Extra-compartmental	86 (72.3 %)
Vertebral compression	
No	80 (67.2 %)
Yes	39 (32.8 %)
Multi-vertebral involvement	
No	60 (50.4 %)
Yes	59 (49.6 %)
Recurrence	
No	92 (77.3 %)
Yes	27 (22.7 %)
Follow-up time (month)	
Median (IQR)	36 (28.5 – 56.0)

Note: IQR, inter-quartile range. Percentages in parentheses represent the proportion of the entire cohort.

Table 2
Differences in the recurrence and non-recurrence groups.

Characteristics	Non-recurrence (N = 92)	Recurrence (N = 27)	*P* value
Age (IQR)	42.5 (27.0–55.0)	37 (24.25–45.75)	0.166
Gender (Female)	53 (57.6 %)	14 (51.9 %)	0.598
Location			0.599
Cervical	15 (16.3 %)	1 (3.7 %)	
Thoracic	31 (33.7 %)	14 (51.6 %)	
Lumbar	23 (25.0 %)	4 (14.8 %)	
Sacrococcygeal	23 (25.0 %)	8 (29.6 %)	
Enneking stage (Extra)	63 (68.5 %)	23 (85.2 %)	0.090
Vertebral compression	24 (26.1 %)	15 (55.56 %)	0.004*
Multi-vertebral involvement	43 (46.7 %)	16 (59.3 %)	0.256
Fractal Dimension	1.30	1.32	0.623
Skewness	−0.485	−0.250	0.019*
Kurtosis	3.34	5.09	0.003*
Entropy	3.29	3.38	0.167
Max-ADC	2482	2119	0.003*
Mean-ADC	1374	1012	<0.0001*
Percentage of the ADC			
10 % ADC	1175	1135	0.628
25 % ADC	1290	1246	0.374
50 % ADC	1559	1393	0.002*
75 % ADC	1950	1744	0.002*
90 % ADC	2187	1999	0.069

Note: Percentages in parentheses represent the proportion of each cohort. ADC, apparent diffusion coefficient, expressed as 10^{-6} mm^2/s; *Significant difference at $p < 0.05$.

entropy. For the parameters of the different percentiles of the ADC compared, the max, mean, 50 % and 75 % percentiles ADC values significantly differed between the two groups. Fig. 2 shows the comparison of preoperative whole-tumor ADC histogram parameters between recurrence and non-recurrence groups.

3.3. Interobserver agreement

The interobserver agreement was moderate to excellent for fractal dimension and all ADC histogram parameters measured by 2 radiologists, with ICCs ranged from 0.777 to 0.985 (Table 3).

3.4. Performance of significant ADC histogram metrics and cut-off values

For parameters with statistical differences between the two groups, the AUC ranged from 0.648 to 0.829. Skewness and Kurtosis showed good specificity (0.826 and 0.946, respectively) but insufficient sensitivity (0.444 and 0.370, respectively). Mean-ADC was the best diagnostic parameter with a Youden index of 0.506, sensitivity of 0.593 and specificity of 0.913. Detailed cutoff values, Youden index, sensitivity and specificity are given in Table 4.

3.5. Diagnostic performance of different risk stratification methods

Logistic regression of histogram parameters showed that skewness, max and mean ADC values were an independent risk factor for recurrence. Detailed results are shown in Table 5. The AUC of the ADC histogram prediction model was 0.871 (95 %CI: 0.797–0.925). As for the clinical model, Enneking staging (OR: 3.572; 95 %CI: 1.061–12.03; $P = 0.04$) and vertebral compression (OR: 4.302; 95 %CI: 1.688–10.961; $P = 0.002$) derived from routine imaging were independent predictors of recurrence. The AUC of the clinical prediction model was 0.704 (95 %CI: 0.614–0.784). Logistic regression of all variables showed that the Enneking stage, mean and 50 % ADC values were independent risk factors. The AUC of the combined prediction model was 0.884 (95 %CI: 0.813–0.935). Through the DeLong test, the AUC of the established ADC histogram and combined models was significantly greater than that of the clinical prediction model (Fig. 3) with P-values of 0.004 and 0.001, respectively. The AUC between the clinical prediction model and the ADC histogram model was not statistically different ($P = 0.606$). Two couples of patient cases are shown in Figs. 4 and 5.

4. Discussion

This study showed that the ADC histogram analysis based on pretreatment DWI has incremental prognostic value in aggressive spine tumors. Skewness, maximum, and mean ADC value of the ADC histogram were an independent risk factor for recurrence. The performance of the ADC histogram model combining these quantitative parameters was significantly improved compared with the clinical model ($P = 0.871$ vs. 0.704, $P < 0.05$).

The treatment of primary spine tumors is a complex and challenging task. The combination of the low prevalence, the complexity of preoperative decision-making, and the demanding surgical procedures emphasize the importance of precise and accurate prediction of the risk of recurrence, which could pave the way for future personalized follow-up treatment and help to select appropriate treatment options for patients. However, prognostic tools for recurrence prediction in primary spinal tumors remain unresolved. Preoperative MR Imaging plays an important role in the evaluation of tumor heterogeneity. Preoperative fractal dimension analysis had been used for the diagnosis and personalized evaluation of the tumor, such as in gastrointestinal stromal tumors [17], prostate cancer [20,21], and brain tumors [22]. Increased FD was frequently associated with increased tumor aggressiveness or poor prognosis. In this study, the difference in FD between recurrence and non-recurrence groups was not significant, which may be due to irregularities in the inherent structure of the spine, such as the pedicle and appendages.

To create meaningful reference tools, promising progress in tumor risk stratification has been made via the use of DWI/ADC in recent years [23,24]. Functional and microscopic differences in the composition of the tumor lesion might be relevant to the development of cancer treatment strategies, as reflected in changes in morphology, histogram shape, and asymmetry. In this study, we found that there was significant difference in skewness between relapse group and non-recurrence group significant differences, which suggested that ADC distribution is more

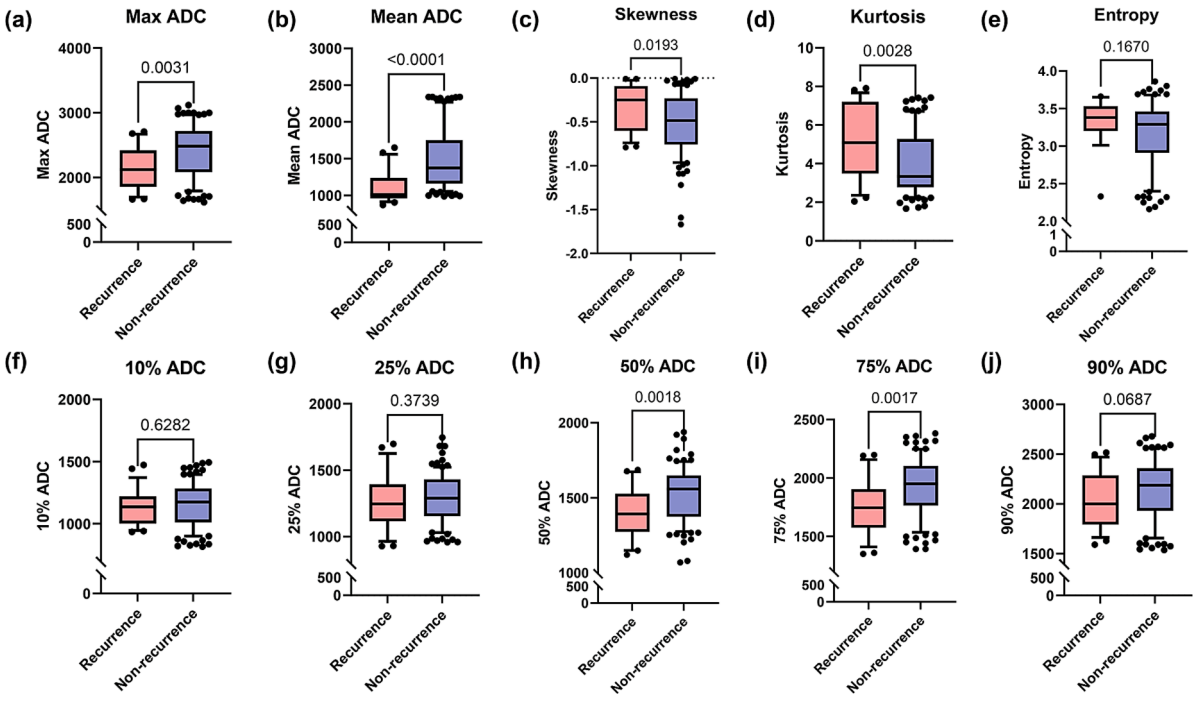

Fig. 2. Box plots showing the distribution of (a) Max ADC, (b) Mean ADC, (c) Skewness, (d) Kurtosis, (e) Entropy, (f) 10 % ADC, (g) 25 % ADC, (h) 50 % ADC, (i) 75 % ADC, and (j) 90 % ADC values between recurrence (n = 27) and non-recurrence (n = 92) groups. P-values indicate the significance of differences between groups for each parameter (*, P < 0.05).

Table 3
Interobserver agreement (ICC) for parameter of fractal and ADC histogram analysis.

Parameter	ICC	95 % Confidence Interval
Fractal Dimension	0.821	0.757–0.869
Skewness	0.985	0.978–0.989
Kurtosis	0.980	0.972–0.986
Entropy	0.777	0.713–0.829
Max-ADC	0.891	0.852–0.921
Mean-ADC	0.973	0.962–0.981
Percentage of the ADC		
10th	0.823	0.756–0.872
25th	0.801	0.737–0.851
50th	0.898	0.859–0.926
75th	0.823	0.756–0.872
90th	0.814	0.771–0.849

Note: ADC, apparent diffusion coefficient, expressed as 10^{-6} mm^2/s.

asymmetric in patients with high risk of recurrence. Previous studies also demonstrated that skewness was a reliable heterogeneity marker in various solid tumors, such as glioblastomas and gliomas [25], pancreatic adenocarcinoma [26], neuroendocrine tumors and endometrial cancer [27], and serous ovarian cancer [28].

In tumors, ADC histograms frequently exhibit non-normal distributions as a result of necrotic, fibrotic, or edematous regions. Utilizing fixed percentiles provides a standardized approach across various tumor types and mitigates distortions in highly skewed distributions [29]. The results of our study show that among the ADC histogram indicators evaluated between the recurrence and non-recurrence groups, the mean value, maximum value, 50th and 75th percentiles showed significant differences between the groups. The observed negative correlation between cell density and ADC suggests that tumors with a higher cell density may have an increased risk of postoperative recurrence. This finding was consistent with the findings in prostate cancer and glioblastoma, in which decreased survival [30] and greater aggressiveness [31] correlated with lower pretreatment ADC. Among them, the mean ADC has the best diagnostic performance, and mean ADC $\leq 1048 \times 10^{-3}$ mm^2/s can be used to predict recurrence. This is a parameter that can be easily and directly obtained in clinical work and picture archiving and communication system, which may represent a promising application of ADC parameters as a non-invasive "histological" method. Our study also performed a robustness test which suggesting the reproducibility of ADC histogram indicators [32–34].

This study had some limitations. First, selection bias could have been introduced because of its two-center, retrospective nature and small sample size. There are currently no large-scale public data sets for primary tumors of the spine, which is a direction that needs further effort. Second, our approach was to compute 2D-FD values for each MRI slice instead of 3D values. Third, we utilized different MRI scanners because of the relatively long study period, which might have had an impact on the values of the ADC parameters, but was not expected to introduce a

Table 4
Diagnostic performance of significant ADC histogram metrics with cut-off values.

Parameters	Cut-off value	Youden Index	Sensitivity (%)	Specificity (%)	AUC (95 % CI)	P
Skewness	>-0.17	0.271	44.44	82.61	0.648 (0.556 – 0.733)	0.014
Kurtosis	>6.91	0.316	37.04	94.57	0.688 (0.596 – 0.769)	0.003
Max-ADC	≤2442	0.347	81.48	53.26	0.686 (0.594 – 0.768)	0.001
Mean-ADC	≤1048	0.506	59.26	91.30	0.829 (0.749 – 0.892)	<0.0001
50 %ADC	≤1442	0.426	74.07	68.48	0.695 (0.604 – 0.776)	0.001
75 %ADC	≤1848	0.415	74.07	67.39	0.696 (0.605 – 0.777)	0.001

Note: ADC, apparent diffusion coefficient, expressed as 10^{-6} mm^2/s; CI, Confidence interval.

Table 5
Prediction models with clinical and ADC histogram parameters.

Clinical Prediction Model				ADC histogram Prediction Model				Combined Prediction Model			
Parameters	**OR**	**95 % CI**	***P* value**	**Parameters**	**OR**	**95 % CI**	***P* value**	**Parameters**	**OR**	**95 % CI**	***P* value**
Enneking stage	3.572	1.061–12.030	0.040*	*Skewness*	6.597	1.187–36.671	0.031	*Enneking stage*	8.469	2.100–34.153	0.003
Vertebral compression	4.302	1.688—10.961	0.002*	*Mean ADC*	0.996	0.992–0.998	0.0004	*Mean ADC*	0.994	0.991–0.997	0.0001
				50 % ADC	0.996	0.993–0.999	0.012	*50 % ADC*	0.996	0.992–0.999	0.008

Note: FD, fractal dimension; PCT, percentage; ADC, apparent diffusion coefficient; OR, odds ratio; CI, confidence interval.

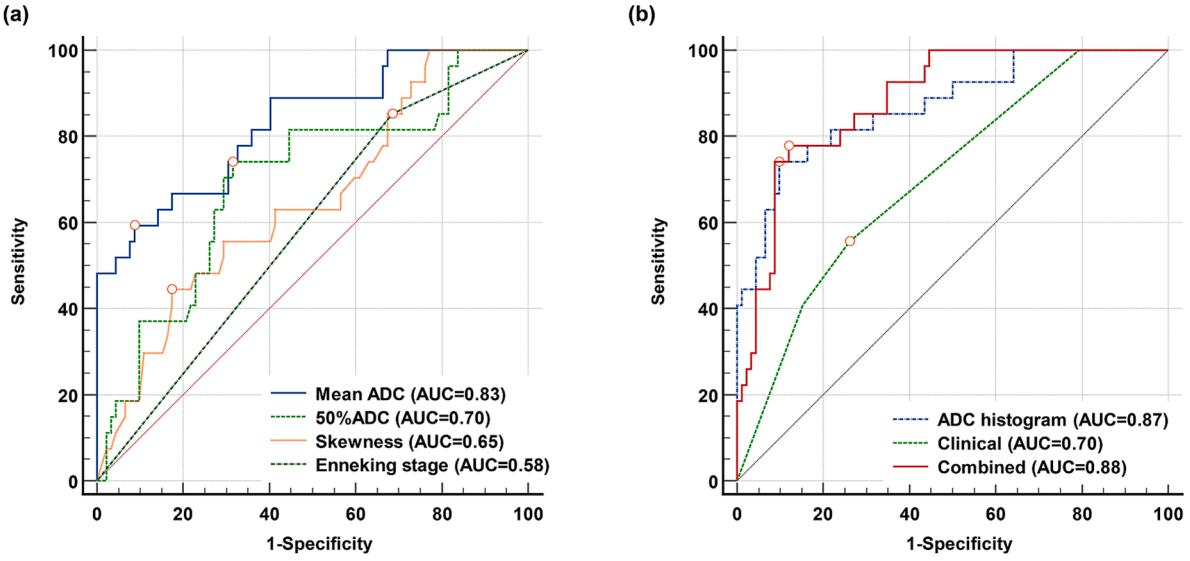

Fig. 3. Receiver operating characteristic curves of the characteristics and three prediction models for postoperative recurrence prediction. ADC, apparent diffusion coefficient; AUC, the area under the curve.

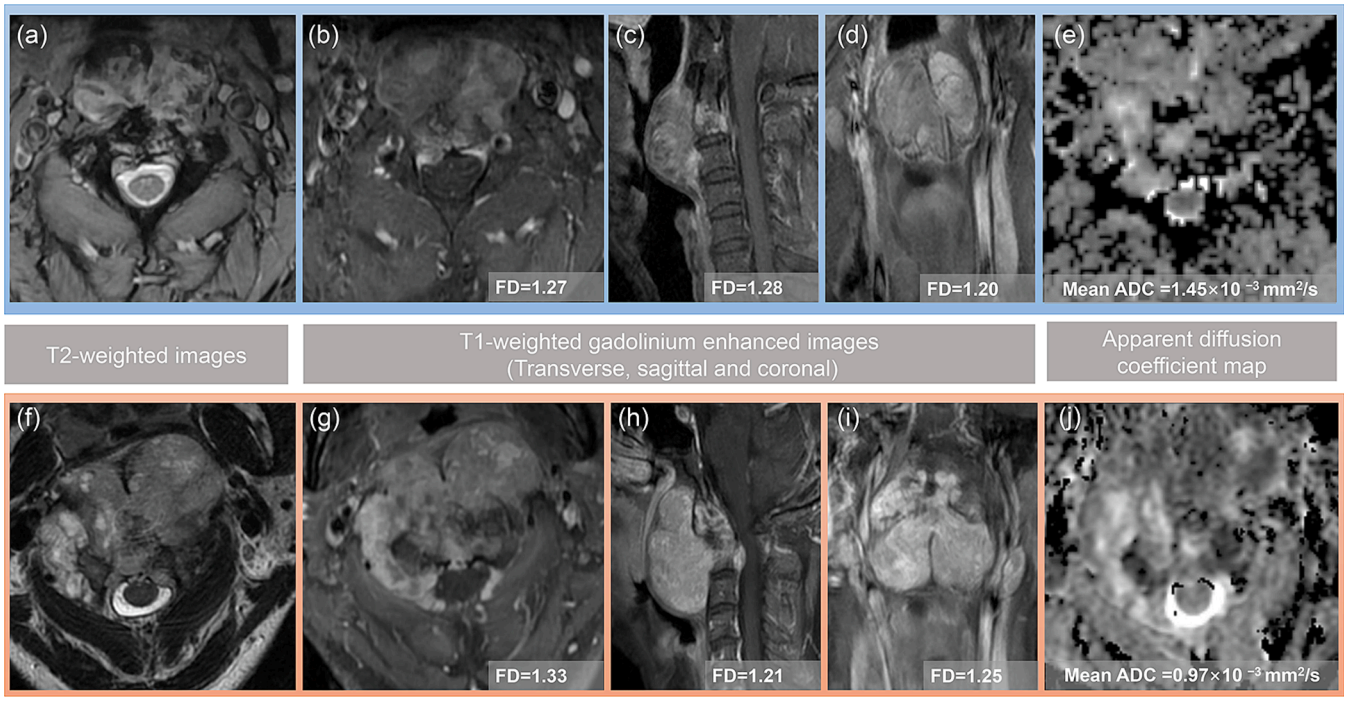

Fig. 4. MRI images of two cases with pathologically confirmed chordoma. (a-e) A 49-year-old male, and no recurrence was observed after 5 years of follow-up; (f-j) A 43-year-old male, was diagnosed with tumor recurrence 11 months after surgery. The FD and mean ADC of the shown layer are listed. Compared to FD, ADC values showed a more noticeable decrease. FD, fractal dimension; ADC, apparent diffusion coefficient.

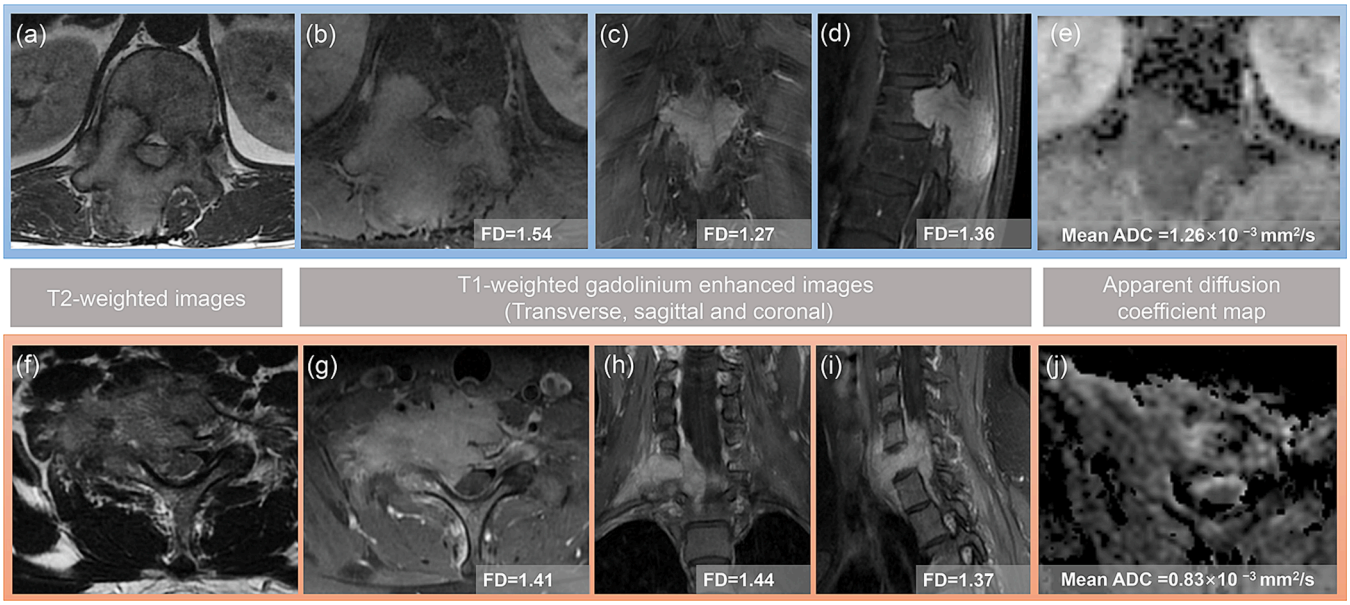

Fig. 5. MRI images of two cases with pathologically confirmed giant cell tumor of bone. (a-e) A 29-year-old male, no recurrence was found at 30 months follow-up; (f-j) A 23-year-old male, tumor recurrence was confirmed 5 months after surgery. The FD and mean ADC of the shown layer are listed. Compared to FD, ADC values showed a more noticeable decrease. FD, fractal dimension; ADC, apparent diffusion coefficient.

major bias. In addition, skewness does not depend on sequence specifics and field strength [35]. Forth, our objective was to assess the feasibility of using presurgical features to predict spinal tumor recurrence, focusing on radiographic parameters, which did not include some clinical examinations or specific treatments. Lastly, although the concept of using ADC histogram model to obtain immediate and noninvasive preoperative prediction of spinal tumor recurrence according to routine clinical settings is appealing, further investigations should focus on larger-sized cohorts and clinical trials.

5. Conclusion

Our findings indicate that quantitative ADC parameters, including skewness, mean, and 50th percentiles of the ADC, should be emphasized in the risk stratification of patients with primary spinal tumors. By comparing the diagnostic performance, the ADC histogram model performed better than the clinical model and can effectively predicted postoperative recurrence. Future individualized follow-up protocols may benefit from incorporating the ADC histogram prediction model, allowing for better selection of patients with aggressive primary spinal tumors for appropriate clinical interventions.

6. Consent for publication

Written informed consent for publication of the clinical details and/or clinical images was obtained from the patient. A copy of the consent form is available for review by the Editor of this journal.

7. Availability of data and materials

The datasets generated during and/or analyzed during the current study are available from the corresponding author on reasonable request.

8. Ethics approval and consent to participate

All procedures were performed in compliance with relevant laws and institutional guidelines and have been approved by the Ethics Committee of Peking University Third Hospital (M2023827). The privacy rights of human subjects have been observed and informed consent was waived.

CRediT authorship contribution statement

Qizheng Wang: Writing – review & editing, Writing – original draft, Validation, Methodology, Investigation, Formal analysis, Data curation, Conceptualization. **Yongye Chen:** Writing – review & editing, Writing – original draft, Visualization, Methodology, Investigation, Formal analysis, Data curation, Conceptualization. **Guangjin Zhou:** Writing – review & editing, Writing – original draft, Supervision, Methodology, Investigation, Formal analysis, Data curation, Conceptualization. **Tongyu Wang:** Writing – original draft, Methodology, Investigation, Formal analysis, Data curation. **Jingchao Fang:** Validation, Software, Investigation, Data curation, Conceptualization. **Ke Liu:** Writing – review & editing, Methodology, Formal analysis, Data curation. **Siyuan Qin:** Writing – review & editing, Validation, Resources, Formal analysis. **Weili Zhao:** Writing – review & editing, Writing – original draft, Validation, Resources, Formal analysis. **Dapeng Hao:** Writing – review & editing, Writing – original draft, Supervision, Resources, Project administration, Investigation, Data curation. **Ning Lang:** Writing – review & editing, Writing – original draft, Supervision, Project administration, Investigation, Funding acquisition, Formal analysis, Conceptualization.

Funding

This work was supported by the National Natural Science Foundation of China [grant numbers 82371921].

Declaration of competing interest

The authors declare the following financial interests/personal relationships which may be considered as potential competing interests: Ning Lang reports financial support was provided by National Natural Science Foundation of China. If there are other authors, they declare that they have no known competing financial interests or personal relationships that could have appeared to influence the work reported in this paper.

References

[1] D.L. Kerr, B.L. Dial, A.L. Lazarides, A.A. Catanzano, W.O. Lane, D.G. Blazer 3rd, B. E. Brigman, S. Mendoza-Lattes, W.C. Eward, M.E. Erickson, Epidemiologic and survival trends in adult primary bone tumors of the spine, Spine J. 19 (12) (2019) 1941–1949.

[2] Z. Zhou, X. Wang, Z. Wu, W. Huang, J. Xiao, Epidemiological characteristics of primary spinal osseous tumors in Eastern China, World J. Surg. Oncol. 15 (1) (2017) 73.

[3] R. Williams, M. Foote, H. Deverall, Strategy in the surgical treatment of primary spinal tumors, Global Spine J. 2 (4) (2012) 249–266.

[4] A.E. Ropper, K.S. Cahill, J.W. Hanna, E.F. McCarthy, Z.L. Gokaslan, J.H. Chi, Primary vertebral tumors: a review of epidemiologic, histological and imaging findings, part II: locally aggressive and malignant tumors, Neurosurgery 70(1) (2012) 211-9; discussion 219.

[5] I. Chong, Q. Ostrom, B. Khan, D. Dandachi, N. Garg, A. Kotrotsou, R. Colen, F. Moron, Whole tumor histogram analysis using DW MRI in primary central nervous system lymphoma correlates with tumor biomarkers and outcome, Cancers (Basel) 11 (10) (2019).

[6] A. Gao, H. Zhang, X. Yan, S. Wang, Q. Chen, E. Gao, J. Qi, J. Bai, Y. Zhang, J. Cheng, Whole-tumor histogram analysis of multiple diffusion metrics for glioma genotyping, Radiology 302 (3) (2022) E16.

[7] X. Ma, X. Ren, M. Shen, F. Ma, X. Chen, G. Zhang, J. Qiang, Volumetric ADC histogram analysis for preoperative evaluation of LVSI status in stage I endometrioid adenocarcinoma, Eur. Radiol. 32 (1) (2022) 460–469.

[8] A. Panda, V.C. Obmann, W.C. Lo, S. Margevicius, Y. Jiang, M. Schluchter, I.J. Patel, D. Nakamoto, C. Badve, M.A. Griswold, I. Jaeger, L.E. Ponsky, V. Gulani, MR fingerprinting and ADC mapping for characterization of lesions in the transition zone of the prostate gland, Radiology 292 (3) (2019) 685–694.

[9] Q.Z. Wang, E.L. Zhang, X.Y. Xing, M.Y. Su, N. Lang, Clinical significance of preoperative CT and MR imaging findings in the prediction of postoperative recurrence of spinal giant cell tumor of bone, Orthop. Surg. 13 (8) (2021) 2405–2416.

[10] A. Spiessberger, N. Dietz, V. Arvind, M. Nasim, B. Gruter, E. Nevzati, S. Hofer, S. K. Cho, Spondylectomy in the treatment of neoplastic spinal lesions - a retrospective outcome analysis of 582 patients using a patient-level meta-analysis, J. Craniovertebr. Junction Spine 12 (2) (2021) 107–116.

[11] P. Chan, S. Boriani, D.R. Fourney, R. Biagini, M.B. Dekutoski, M.G. Fehlings, T.C. Ryken, Z.L. Gokaslan, F.D. Vrionis, J.S. Harrop, M.H. Schmidt, L.R. Vialle, P.C. Gerszten, L.D. Rhines, S.L. Ondra, S.R. Pratt, C.G. Fisher, An assessment of the reliability of the Enneking and Weinstein-Boriani-Biagini classifications for staging of primary spinal tumors by the Spine Oncology Study Group, Spine (Phila Pa 1976) 34(4) (2009) 384-91.

[12] W. Xu, X. Li, W. Huang, Y. Wang, S. Han, S. Chen, L. Xu, X. Yang, T. Liu, J. Xiao, Factors affecting prognosis of patients with giant cell tumors of the mobile spine: retrospective analysis of 102 patients in a single center, Ann. Surg. Oncol. 20 (3) (2013) 804–810.

[13] M.Y. Marusina, A.P. Mochalina, E.P. Frolova, V.I. Satikov, A.A. Barchuk, V. I. Kuznetcov, V.S. Gaidukov, S.A. Tarakanov, MRI image processing based on fractal analysis, Asian Pac. J. Cancer Prev. 18 (1) (2017) 51–55.

[14] J. Wang, Y. Li, F. Yang, L. Bravo, K. Wan, Y. Xu, W. Cheng, J. Sun, Y. Zhu, T. Zhu, G.V. Gkoutos, Y. Han, Y. Chen, Fractal analysis: prognostic value of left ventricular trabecular complexity cardiovascular MRI in participants with hypertrophic cardiomyopathy, Radiology 298 (1) (2021) 71–79.

[15] F. Michallek, M.A. Haouari, O. Dana, A. Perrot, S. Silvera, A. Dallongeville, M. Dewey, M. Zins, Fractal analysis improves tumour size measurement on computed tomography in pancreatic ductal adenocarcinoma: comparison with gross pathology and multi-parametric MRI, Eur. Radiol. 32 (8) (2022) 5053–5063.

[16] T. Tochigi, S.C. Kamran, A. Parakh, Y. Noda, B. Ganeshan, L.S. Blaszkowsky, D. P. Ryan, J.N. Allen, D.L. Berger, J.Y. Wo, T.S. Hong, A. Kambadakone, Response prediction of neoadjuvant chemoradiation therapy in locally advanced rectal cancer using CT-based fractal dimension analysis, Eur. Radiol. 32 (4) (2022) 2426–2436.

[17] Y. Kurata, K. Hayano, G. Ohira, K. Narushima, T. Aoyagi, H. Matsubara, Fractal analysis of contrast-enhanced CT images for preoperative prediction of malignant potential of gastrointestinal stromal tumor, Abdom. Radiol. (NY) 43 (10) (2018) 2659–2664.

[18] M.U. Jawad, S.P. Scully, In brief: classifications in brief: enneking classification: benign and malignant tumors of the musculoskeletal system, Clin. Orthop. Relat. Res. 468 (7) (2010) 2000–2002.

[19] F. Michallek, M. Dewey, Fractal analysis in radiological and nuclear medicine perfusion imaging: a systematic review, Eur. Radiol. 24 (1) (2014) 60–69.

[20] F. Michallek, H. Huisman, B. Hamm, S. Elezkurtaj, A. Maxeiner, M. Dewey, Prediction of prostate cancer grade using fractal analysis of perfusion MRI: retrospective proof-of-principle study, Eur. Radiol. 32 (5) (2022) 3236–3247.

[21] F. Michallek, H. Huisman, B. Hamm, S. Elezkurtaj, A. Maxeiner, M. Dewey, Accuracy of fractal analysis and PI-RADS assessment of prostate magnetic resonance imaging for prediction of cancer grade groups: a clinical validation study, Eur. Radiol. 32 (4) (2022) 2372–2383.

[22] D. Battalapalli, S. Vidyadharan, B. Prabhakar Rao, P. Yogeeswari, C. Kesavadas, V. Rajagopalan, Fractal dimension: analyzing its potential as a neuroimaging biomarker for brain tumor diagnosis using machine learning, Front. Physiol. 14 (2023) 1201617.

[23] V. Koutoulidis, E. Terpos, N. Papanikolaou, S. Fontara, I. Seimenis, M. Gavriatopoulou, I. Ntanasis-Stathopoulos, C. Bourgioti, J. Santinha, J. M. Moreira, E. Kastritis, M.A. Dimopoulos, L.A. Moulopoulos, Comparison of MRI features of fat fraction and ADC for Early treatment response assessment in participants with multiple myeloma, Radiology 304 (1) (2022) 137–144.

[24] C. Reinhold, S. Nougaret, Radiomic ADC metrics as a tool to better understand tumor biology, Radiol. Imaging Cancer 2 (3) (2020) e200051.

[25] N. Just, Improving tumour heterogeneity MRI assessment with histograms, Br. J. Cancer 111 (12) (2014) 2205–2213.

[26] R. De Robertis, L. Tomaiuolo, F. Pasquazzo, L. Geraci, G. Malleo, R. Salvia, M. D'Onofrio, Correlation BETWEEN ADC histogram-derived metrics and the time to metastases in resectable pancreatic adenocarcinoma, Cancers (Basel) 14 (24) (2022).

[27] J. Zhang, X. Yu, X. Zhang, S. Chen, Y. Song, L. Xie, Y. Chen, H. Ouyang, Whole-lesion apparent diffusion coefficient (ADC) histogram as a quantitative biomarker to preoperatively differentiate stage IA endometrial carcinoma from benign endometrial lesions, BMC Med. Imaging 22 (1) (2022) 139.

[28] J. Lu, H.M. Li, S.Q. Cai, S.H. Zhao, F.H. Ma, Y.A. Li, X.L. Ma, J.W. Qiang, Prediction of platinum-based chemotherapy response in advanced high-grade serous ovarian cancer: ADC histogram analysis of primary tumors, Acad. Radiol. 28 (3) (2021) e77–e85.

[29] P. LaViolette, N. Mickevicius, E. Cochran, S. Rand, J. Connelly, J. Bovi, M. Malkin, W. Mueller, K. Schmainda, Precise ex vivo histological validation of heightened cellularity and diffusion-restricted necrosis in regions of dark apparent diffusion coefficient in 7 cases of high-grade glioma, Neuro Oncol. 16 (12) (2014) 1599–1606.

[30] Y.S. Choi, S.S. Ahn, D.W. Kim, J.H. Chang, S.G. Kang, E.H. Kim, S.H. Kim, T. H. Rim, S.K. Lee, Incremental prognostic value of ADC histogram analysis over MGMT promoter methylation status in patients with glioblastoma, Radiology 281 (1) (2016) 175–184.

[31] A. Hoang Dinh, C. Melodelima, R. Souchon, J. Lehaire, F. Bratan, F. Mege-Lechevallier, A. Ruffion, S. Crouzet, M. Colombel, O. Rouviere, Quantitative analysis of prostate multiparametric MR images for detection of aggressive prostate cancer in the peripheral zone: a multiple imager study, Radiology 280 (1) (2016) 117–127.

[32] K. Onodera, M. Hatakenaka, N. Yama, M. Onodera, T. Saito, T.C. Kwee, T. Takahara, Repeatability analysis of ADC histogram metrics of the uterus, Acta Radiol. 60 (4) (2019) 526–534.

[33] D.C. Newitt, G. Amouzandeh, S.C. Partridge, H.S. Marques, B.A. Herman, B. D. Ross, N.M. Hylton, T.L. Chenevert, D.I. Malyarenko, Repeatability and reproducibility of ADC histogram metrics from the ACRIN 6698 breast cancer therapy response trial, Tomography 6 (2) (2020) 177–185.

[34] T. Barrett, E.M. Lawrence, A.N. Priest, A.Y. Warren, V.J. Gnanapragasam, F. A. Gallagher, E. Sala, Repeatability of diffusion-weighted MRI of the prostate using whole lesion ADC values, skew and histogram analysis, Eur. J. Radiol. 110 (2019) 22–29.

[35] K. Drevelegas, K. Nikiforaki, M. Constantinides, N. Papanikolaou, L. Papalavrentios, I. Stoikou, P. Zarogoulidis, G. Pitsiou, A. Pataka, J. Organtzis, E. Papadaki, K. Porpodis, I. Kougioumtzi, I. Kioumis, C. Kouskouras, E. Akriviadis, A. Drevelegas, Apparent diffusion coefficient quantification in determining the histological diagnosis of malignant liver lesions, J. Cancer 7 (6) (2016) 730–735.